International Journal of Networking and Computing – www.ijnc.org, ISSN 2185-2847
Volume 16, Number 2, pages 77–98, July 2026

Enhancing Smart Tourism in Mountainous Areas with BLE Beacon and GNSS-Based Proximity Detection

Sho Kato
Graduate School of Regional Development and Creativity, Utsunomiya University
Yoto 7-1-2, Utsunomiya, Tochigi, 321-8585, JAPAN

Madoka Hasegawa
School of Engineering, Utsunomiya University
Yoto 7-1-2, Utsunomiya, Tochigi, 321-8585, JAPAN

Naoya Tsuruta
School of Engineering, Utsunomiya University
Yoto 7-1-2, Utsunomiya, Tochigi, 321-8585, JAPAN

and

Atsushi Ito
Faculty of Economics, Chuo University
Higashinakano 742-1, Hachioji, Tokyo, 192-0393, JAPAN

Received: February 20, 2026
Revised: May 3, 2026
Accepted: June 1, 2026
Communicated by Shuichi Ichikawa

Abstract

Accurate positioning in mountainous and forested environments remains challenging for tourist assistance applications. This study proposes a hybrid proximity detection method that integrates Global Navigation Satellite System (GNSS) gating with Bluetooth Low Energy (BLE) refinement. The system first detects the user's approach using GNSS and then estimates the point of closest approach based on BLE RSSI variations or packet reception counts. Experiments were conducted at the Senjogahara Nature Exploration Trail in Nikko, Japan, which includes both forested sections and flat open areas. In Senjogahara, GNSS achieved the highest positioning accuracy under normal conditions; however, its performance degraded under dense forest canopy. Even in such conditions, the hybrid method incorporating BLE-based refinement maintained more stable performance than the GNSS-only approach. Additional experiments were also conducted in a flat urban area, specifically at a university rugby field. In these experiments, the proposed method using a BLE reception-count trigger achieved the smallest positioning error, outperforming both the BLE-only and GNSS-only methods.

Keywords: BLE beacon, GNSS, proximity detection, sensor fusion, location-based services, tourism application

1 Introduction

Location-based services (LBS) have become a key technological foundation for enhancing tourist experiences by providing navigation, contextual information, and safety guidance[1]. In natural parks and mountainous regions, mobile applications are expected to support route planning and situational awareness while operating under severe infrastructural constraints. However, cellular connectivity in such environments is often limited or unavailable, making it essential to develop positioning techniques that operate robustly without relying on continuous network access.

Bluetooth Low Energy (BLE) beacons have been widely adopted for indoor navigation systems, museum guidance, and cultural heritage applications[2] owing to their low cost, low power consumption, and offline capability. Despite these advantages, BLE-based proximity detection suffers from signal instability caused by terrain, vegetation, weather conditions, and multipath effects. Consequently, estimation based on the Received Signal Strength Indicator (RSSI) values of BLE signals becomes unreliable in outdoor forest environments.

Conversely, Global Navigation Satellite Systems (GNSS) generally provide higher accuracy in open areas, but their performance deteriorates under forest canopy —particularly in mountainous regions— due to reduced satellite visibility and multipath interference. Additionally, GNSS positioning can be severely degraded by geophysical disturbances such as solar flares, occasionally producing tens of meters of positioning error. These limitations indicate that relying solely on BLE or GNSS is insufficient for delivering accurate proximity-based information in diverse outdoor environments.

Sensor fusion approaches that combine GNSS, BLE, inertial sensors, and other modalities have recently attracted attention as a means of overcoming the shortcomings of single-modality positioning. However, existing studies primarily focus on indoor or urban settings, where signal conditions are more consistent and device power constraints are relatively minor. In contrast, outdoor deployments in mountainous tourist areas face unique challenges: BLE beacons must operate under strict power constraints (often solar-powered), beacon transmission intervals tend to be long, and environmental variability is substantial. Moreover, few studies have systematically evaluated fusion-based proximity detection on real-world tourist trails, where GNSS degradation may occur unpredictably due to atmospheric disturbances.

Given these challenges, robust proximity detection for outdoor tourism applications requires a hybrid approach that accommodates environmental variability, device limitations, and real-world deployment conditions. To address this need, we focus on Senjogahara, a forest–wetland region in Nikko, Japan, and the smartphone application *Oku-nikko Navi*, which provides offline tourist information using BLE beacons installed along hiking trails.

Building on this context, we pose the following research question:

> Can a hybrid proximity-detection framework that integrates GNSS-based coarse gating with BLE-based short-range refinement achieve more reliable and accurate proximity detection than GNSS-only and BLE-only approaches in forested and mountainous outdoor environments?

Specifically, we examine:

1. whether BLE-based triggering remains robust under long advertising intervals and substantial RSSI fluctuations commonly observed in outdoor environments, and
2. whether the hybrid approach can maintain detection accuracy in situations where GNSS performance degrades due to forest canopy.

Here, a trigger refers to a mechanism that initiates the process of presenting information on a smartphone.

The main contributions of this work are summarized as follows:

- **A hybrid proximity detection framework for outdoor tourism environments.** We propose a two-stage GNSS–BLE hybrid method designed for mountainous and forested regions, and evaluate its feasibility through field experiments.

- **Experimental validation in real-world environments.**The proposed method is evaluated in both urban and forested settings, and its performance is compared with BLE-only and GNSS-only approaches.
- **Analysis of BLE trigger mechanisms under outdoor conditions.**Two BLE-based trigger strategies are examined, and their characteristics are analyzed with respect to environmental variability and system parameters.
- **Practical considerations for deployment in mountainous areas.**We discuss implementation aspects and provide insights into beacon configuration and operational constraints for real-world applications.

The experimental results indicate that the proposed hybrid approach achieves stable performance across different environments and maintains robustness even under degraded GNSS conditions.

The remainder of this paper is organized as follows: Section 2 reviews related work on BLE positioning, GNSS accuracy, and sensor fusion techniques. In Section 3, we describe the environmental conditions of the field site and present the problem setting for this study. Section 4 describes the proposed method. Section 5 details the experimental setup, while Section 6 analyzes the results. Section 7 concludes the paper.

2 Related Work

2.1 BLE-based Positioning

BLE beacons have been widely adopted for proximity detection and indoor navigation due to their low cost and compatibility with commodity smartphones. BLE-based positioning is known to suffer from significant RSSI fluctuations caused by channel behavior and multipath effects [3]. Prior works have investigated several signal features for BLE-based localization, including Received Signal Strength Indicator (RSSI), Angle of Arrival (AoA), and Angle of Departure (AoD). AoA/AoD techniques introduced in Bluetooth 5.1 can achieve sub-meter accuracy when antenna arrays are available [4, 5, 6, 7, 8, 9, 10], but such configurations are impractical for consumer smartphones. Consequently, most BLE-based positioning for smartphones relies on RSSI, despite its well-known sensitivity to multipath propagation, temporal fluctuations, and environmental attenuation.

Indoor BLE positioning studies have shown that signal filtering (e.g., median, Kalman, or particle filtering) significantly reduces RSSI fluctuations and improves localization accuracy [11]. Moreover, RSSI fingerprinting approaches, including KNN- and WKNN-based methods, achieve sub-meter accuracy in various indoor environments [12].

However, fingerprinting requires extensive site surveying and updates, making it unsuitable for large or highly dynamic outdoor environments. Additionally, BLE signal behavior in forests is significantly affected by vegetation density, terrain reflections, beacon transmission intervals, and weather conditions. These limitations motivate hybrid approaches that confine BLE usage to short-range refinement rather than standalone localization.

2.2 GNSS Positioning in Forest Environments

Smartphone GNSS accuracy varies considerably with canopy openness, vegetation density, and atmospheric conditions. Prior work reports that GNSS errors can increase from 2–3 m in open areas to more than 10 m under forest canopy due to reduced satellite visibility and multipath interference [13, 14]. Although recent consumer-grade smartphones increasingly support dual-frequency GNSS, their positioning accuracy remains limited due to hardware constraints such as low-quality antennas and high observation noise.

Furthermore, GNSS signals are vulnerable to geophysical disturbances such as solar flares, which can induce ionospheric irregularities. Solar flare events have been observed to cause abrupt GNSS drift, significantly degrading positioning stability [15]. These constraints indicate that GNSS alone is insufficient for reliable proximity detection in mountainous and forested tourist regions.

(a) Open area

(b) Forest area

Figure 1: Senjogahara nature exploration trail.

2.3 Fusion Approaches for Robust Outdoor Localization

Sensor fusion approaches that combine GNSS, BLE, inertial sensors, Wi-Fi, or ultra-wideband (UWB) aim to overcome the limitations of single-modality positioning. GNSS–BLE hybrid frameworks typically use GNSS for coarse localization and BLE RSSI or reception count for short-range refinement. Prior studies have shown that multimodal fusion can enhance robustness and accuracy by exploiting complementary sensor characteristics [16].

However, most existing studies focus on indoor or urban environments where radio conditions are relatively stable and power constraints are minimal. Outdoor tourist trails pose different challenges: BLE beacons are often solar powered, forcing long transmission intervals; environmental conditions vary widely with weather and vegetation; and GNSS degradation can occur unpredictably. Few studies have systematically evaluated fusion stability in real-world mountainous environments or examined BLE trigger behavior under long-interval outdoor beacon deployments.

2.4 Summary of Research Gap

While prior research has explored the limitations of BLE and GNSS individually and has proposed multimodal approaches, significant gaps remain. In particular, existing studies do not adequately evaluate hybrid GNSS–BLE proximity detection under realistic outdoor conditions involving forest canopy, low-power beacon constraints, weather-induced variability, and geophysical disturbances such as solar flares. Moreover, prior work does not systematically examine BLE trigger design under long beacon transmission intervals, despite its practical importance for sustainable outdoor deployments.

To address these gaps, this study conducts an extensive evaluation of hybrid proximity detection in a challenging forest–wetland environment and proposes trigger mechanisms tailored to the constraints and requirements of outdoor tourism applications.

3 Problem Setting

Figure 1 shows examples of the open and forested environments surrounding the BLE beacons installed along the Senjogahara Nature Exploration Trail. The beacon device and the signposts used in the field are illustrated in Figure 2. All installations were conducted with permission from the Ministry of the Environment and Tochigi Prefecture. The beacons were mounted on top of signposts at heights ranging from approximately 0.5 to 3 m, depending on the size of each signpost.

Figure 3a presents a map of the deployed beacons. A total of 18 BLE beacons were installed. Although the locations are labeled No. 1 through No. 21, beacons are not currently placed at positions No. 3, No. 13, and No. 16. When a user approaches a beacon, the mobile application automatically detects the signal and displays location-specific content on the smartphone (Figure 3b). Because the

(a) BLE beacon.

(b) Interpretive sign (No. 8).

(c) Interpretive sign (No. 11).

(d) Directional sign (No. 21).

Figure 2: BLE beacons and their installation at guide points (beacon locations indicated by red circles).

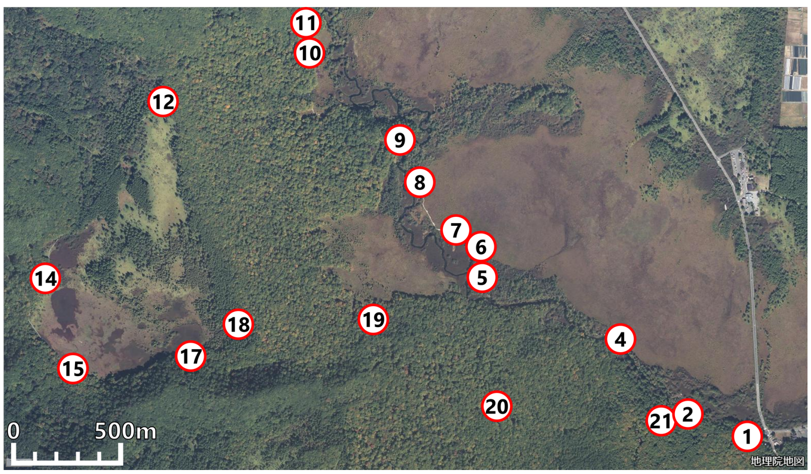

(a) Beacon point.

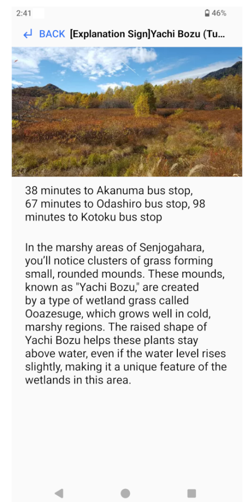

(b) Proximity message at No. 8.

Figure 3: Beacon installation sites and an example proximity message.

Table 1: Location category of each beacon.

Location	Beacon ID
Open areas	4, 6, 7, 8, 9
Forested areas	1, 2, 5, 10, 11, 12, 14, 15, 17, 18, 19, 20, 21

content is preloaded in the application, no network connection is required. The displayed information includes estimated arrival times at nearby bus stops and descriptions of local vegetation.

Table 1 shows the location category of each beacon. Beacons No. 4, 6, 7, 8, and 9 are located in relatively open areas along the boardwalk, while the other beacons are situated within forested areas.

A typical usage scenario for the *Oku-nikko Navi* application is as follows. When a visitor begins walking along the Senjogahara Nature Trail, they launch the application on their smartphone. As the visitor approaches a signpost equipped with a BLE beacon, the application autonomously detects the beacon signal—even when the smartphone is in sleep mode—and provides location-specific information. This mechanism enables visitors to learn about the surrounding vegetation and adjust their route accordingly, thereby enhancing the overall hiking experience. However, providing stable location-based services in mountainous environments is challenging due to the inherent instability of both BLE and GNSS signals. The BLE beacons used in this study are powered by solar cells, and their signal strength and transmission intervals may fluctuate depending on weather conditions, terrain-induced reflections, and hardware failures.

Figure 4a shows the reception distance d for each beacon, defined as the distance between the point at which the smartphone first received the BLE signal and the beacon itself. The error bars in the figure indicate the standard deviation. Distances were measured using a measuring wheel, and measurements were conducted approximately ten times between 2023 and 2024. The exact number of measurements varied across beacons due to occasional device malfunctions. The results indicate substantial variability, with some beacons detected within 10 m and others exceeding 40 m.

As shown in Figure 4a, beacons No. 6-9 in the open area exhibit relatively shorter BLE signal reception distances than those in the forested area. This is because the open-area beacons are installed along a wooden boardwalk in a wetland, where there are few surrounding trees, the terrain is flat, and signal reflections are limited. In contrast, in the forested area, BLE signals are often received at longer distances, typically around 20 m. However, there are also beacons that do not follow this general trend, such as No. 4 in the open area and No. 2 and No. 15 in the forested area.

Figure 4b presents boxplots of the RSSI distributions measured directly in front of each beacon. The whiskers indicate the minimum and maximum values. The figure shows that substantial fluctuations occur even under controlled conditions. These results suggest that proximity detection based solely on RSSI thresholding lacks reliability. The BLE signal RSSI strength measured directly in front of the beacons is strongly influenced by individual beacon characteristics, weather-dependent solar exposure, and battery charge conditions, and no systematic difference is observed between open and non-open areas.

GNSS-based positioning exhibits similar limitations. Accuracy may deteriorate due to reduced satellite visibility, multipath propagation, and occlusions caused by terrain or vegetation. Such factors may lead to delayed or failed proximity detection, thereby impairing timely information delivery and diminishing the practical utility of location-based services in tourism applications. The primary objective of this study is to ensure stable and accurate information delivery within a 5 m radius of each beacon, assuming that adult users walk at a typical pace.

4 Proposed Method

We propose a two-stage proximity detection pipeline that integrates GNSS-based coarse approach detection with BLE-based fine-grained closest-point estimation. Unlike conventional single-modality approaches, the proposed framework explicitly accounts for the unique operational constraints of forested outdoor environments—such as solar-powered beacons with limited energy budgets, long advertising intervals, and intermittent signal availability—and is designed to maintain robustness even under severe variability in radio conditions.

In the proposed method, the user's latitude and longitude are continuously monitored using GNSS, and the distance to each beacon is calculated to identify the beacon closest to the user. When the distance between the user and that beacon falls below a predefined threshold, the system determines that the user has entered a proximity area. Within this proximity area, once a BLE signal that satisfies the specified conditions is received, the information presentation process is triggered and the corresponding information is displayed as a pop-up on the screen. The overall behavior of the system is illustrated in Figure 5.

An architectural overview of the method is illustrated in Figure 6. The proposed method first performs GNSS-based gating and then displays a message on the smartphone indicating that the user has reached the vicinity of the beacon when a BLE signal satisfying the specified conditions is received.

However, as illustrated in Figure 7, if there is an error in the GNSS-estimated smartphone position, a message indicating arrival in the vicinity of the beacon may be displayed at a location farther from the true closest-point position.

The following section provides a detailed, step-by-step description of each stage of the pipeline, clarifying how GNSS-based gating narrows the search region and how BLE triggers refine closest-

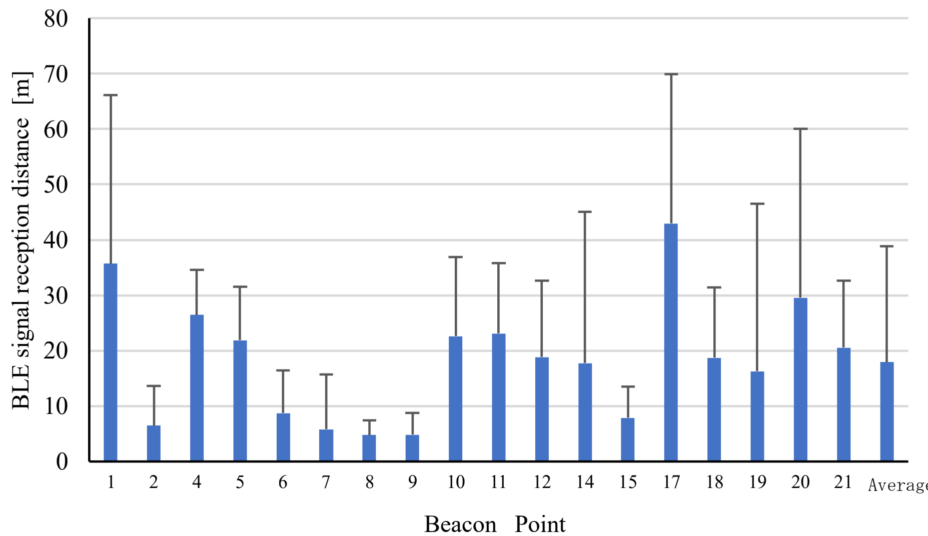

(a) BLE reception distance.

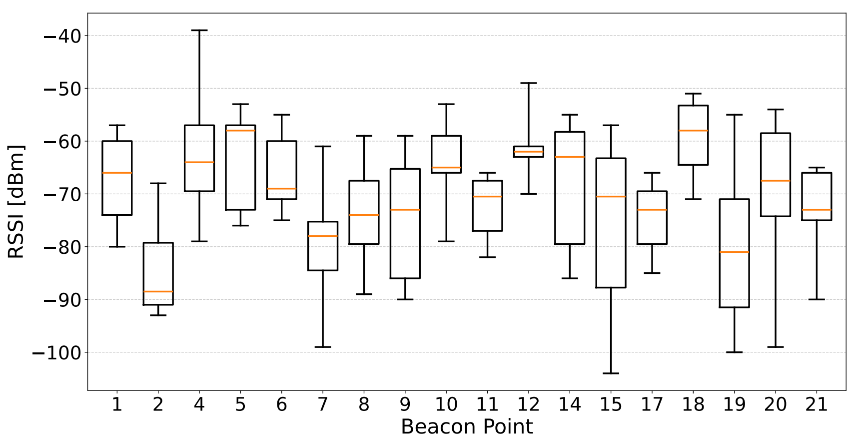

(b) Front-facing RSSI of the beacon.

Figure 4: Instability in beacon behavior.

point detection under challenging environmental and hardware constraints.

4.1 Stage 1: GNSS-based Gating (Approach Detection)

The application computes the geodesic distance d_{GNSS} between the smartphone's current GNSS position and the registered beacon coordinate at approximately 1-second intervals. In our experiments, the beacon coordinates were pre-measured and stored within the application. These coordinates were obtained by computing the centroid of repeated RTK-GNSS measurements, thereby reducing random positional fluctuations and improving reference stability.

When the computed distance satisfies $d_{GNSS} < r$, the system determines the user as being within the near-beacon region and activates the second-stage BLE processing.

Threshold selection. Preliminary field tests showed that a threshold of $r = 5\,\mathrm{m}$ was sufficient

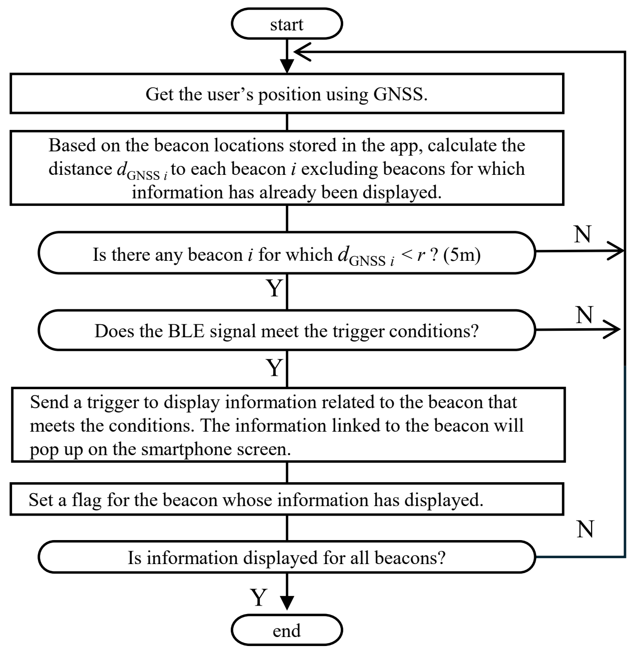

Figure 5: Overall behavior of the proposed system.

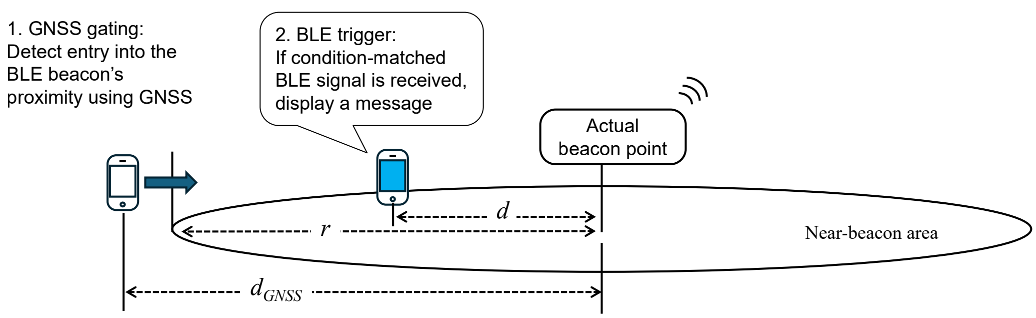

Figure 6: Overview of the proposed method.

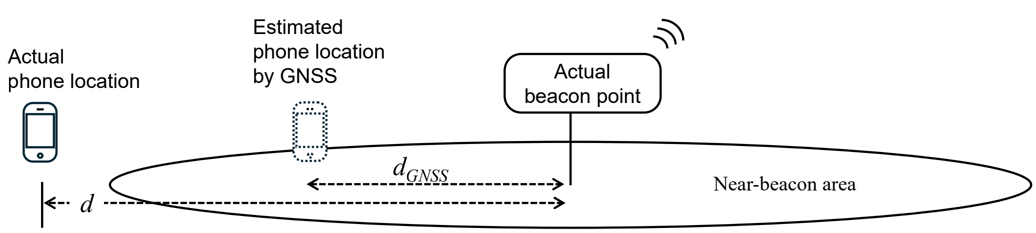

Figure 7: Gating decision errors induced by GNSS inaccuracies.

in flat, unobstructed areas. In contrast, in the Senjogahara area, GNSS accuracy tended to degrade under forest canopy due to reduced satellite visibility and multipath propagation. In such environments, using a threshold larger than 5 m could potentially reduce missed detections. However, increasing the threshold excessively can raise the risk of unintended detections and duplicate information delivery from multiple locations. Considering both the risk of missed detections in forested environments and the increased likelihood of false detections with larger thresholds, we determined that a threshold of 5 m provided the best balance between accuracy and reliability; therefore, we adopted it as the final value.

4.2 Stage 2: BLE Triggers (Closest-Point Determination)

Within the GNSS near-beacon window, BLE signals are employed to refine the closest-point estimation. Two trigger mechanisms were evaluated in our experiments.

1. **Reception-count trigger (received twice)**: The closest point is declared once two BLE receptions are observed within the GNSS near-beacon window. During this interval, the user is assumed to be moving forward toward the beacon; therefore, the reception point obtained within the window provides a more dependable approximation of the true closest approach.

2. **RSSI decrease trigger (single decrease)**: After the user enters the GNSS near-beacon window, the closest point is declared at the moment when the first decrease in RSSI is detected. The decrease is determined from the difference between the current RSSI and the previously received RSSI, where the previous RSSI may have been obtained outside the near-beacon window. This approach aims to capture the earliest indication that the user has passed the point of closest proximity and has begun moving away from the beacon.

   When the user's walking speed is high and the transmission interval is long, the previously described reception-count trigger may allow the user to overshoot the beacon location by a substantial distance. In contrast, the RSSI-decrease method is expected to detect the moment of passage more promptly, as it relies on the first observed downward trend in RSSI.

   However, this expected behavior relies on an idealized monotonic RSSI profile, which rarely holds in real outdoor environments where RSSI frequently fluctuates due to multipath and vegetation. As shown later in our experiments, such fluctuations often cause premature or incorrect trigger activation.

4.3 Analytical Model of the BLE Trigger Reception Position

The BLE trigger reception distance d is defined as the distance between the beacon location and the point at which the BLE trigger condition is satisfied. It represents the systematic latency induced by walking speed, beacon advertising interval, and the trigger mechanism.

Let walking speed v (m/s), beacon transmit interval i (s), and GNSS threshold r (m). In our analysis, we assume an idealized RSSI profile in which the signal strength increases as the user approaches the beacon and decreases after passing the closest point. Although real-world RSSI measurements often exhibit fluctuations due to multipath effects, antenna orientation, and environmental variability, this assumption is used to derive the analytical model. The expected distance d (m) at trigger is approximated by:

$$d \approx r - v \cdot 1.5\, i \quad \text{(received twice)}, \tag{1}$$

$$d \approx v \cdot 0.5\, i \quad \text{(single decrease)}, \tag{2}$$

These coefficients correspond to the expected time-to-event under the assumption that the beacon transmission phase is uniformly distributed. On average, two BLE receptions require approximately $1.5\, i$, and a single RSSI decrease occurs after $0.5\, i$.

Using a representative adult walking speed of $v \approx 1.4\,\text{m/s}$ and a beacon transmission interval of $i = 1.5\,\text{s}$, the expected distance for each trigger mechanism can be quantitatively assessed.

Figure 8 illustrates the relationship between the beacon advertising interval and the resulting absolute distance between the BLE trigger reception position and the beacon installation position, assuming a fixed walking speed of $v = 1.4\,\text{m/s}$. The bands above and below each line in this graph represent the worst-case (upper bound) and best-case (lower bound) conditions, respectively.

This result indicates that RSSI-decrease–based triggers have inherent limitations under long advertising-interval conditions. When beacon transmissions become temporally sparse, the timing of received signals becomes coarse, thereby directly increasing positional uncertainty. Furthermore,

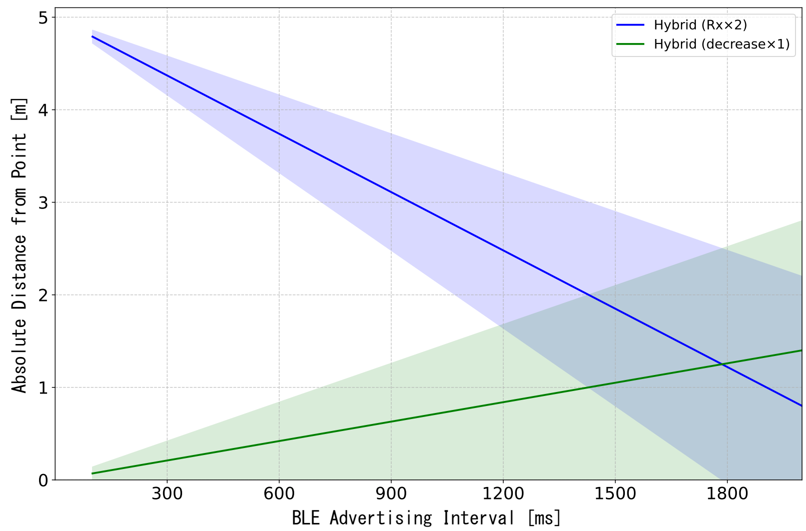

Figure 8: Absolute distance from the beacon at the BLE trigger as a function of the advertising interval ($v = 1.4\,\mathrm{m/s}$).

when the advertising interval is long, trigger methods that rely on detecting multiple consecutive RSSI decreases are expected to become more unstable.

For this reason, detection methods based on two or more consecutive RSSI decreases were excluded from consideration. Based on these findings, this study adopted and compared two trigger methods: the reception-count trigger, which activates when two BLE signals are received, and the RSSI-decrease trigger, which activates when the RSSI decreases once.

4.4 Implementation Notes

BLE beacons. Custom solar-powered BLE beacons (nRF52832, iBeacon protocol, transmission power of +4 dBm) were deployed at each guide point. To balance energy consumption with detection responsiveness, the advertising interval was configured to approximately 1500 ms. In this study, we regard an advertising interval of approximately 1500 ms as a long interval, because typical indoor BLE deployments commonly use intervals in the range of 100-300 ms, and even outdoor deployments for pedestrian applications often adopt sub-second intervals. In contrast, solar-powered beacons in mountainous environments necessitate much longer intervals to conserve energy.

BLE scanning. BLE scanning can technically be performed continuously on Android; however, practical deployment is subject to operating-system constraints related to scan duty cycles and power management. To minimize detection latency, our implementation configures the BLE scanner using `ScanSettings` with the `SCAN_MODE_LOW_LATENCY` option, which is the fastest scan mode supported by the Android BLE framework. This configuration ensures that scan results are delivered immediately without batching, thereby improving the responsiveness of beacon detection.

Nevertheless, Android imposes power-management restrictions when continuous scanning is performed for extended periods, which may cause the operating system to throttle or delay scan operations. To mitigate these effects, the application adopts a periodic restart strategy: after performing continuous scanning for 5 minutes, the scanner is paused for 100 ms and then immediately restarted. By repeating this cycle, the system maintains high-frequency BLE scanning while avoiding OS-level throttling, achieving a balance between responsiveness and energy efficiency.

GNSS updates. GNSS positioning was sampled via the Android Location API at approximately 1 second intervals, providing continuous updates of the user's estimated location. To suppress temporal fluctuations in GNSS accuracy caused by forest canopy attenuation and variations in satellite visibility, a gating mechanism with a distance threshold of 5 m was applied for near-beacon detection.

Each beacon installation point has a signboard, and information that is not shown on the signboard is displayed in the app in conjunction with the beacon. For example, as part of safety-related information, the app shows the distance to the nearest bus stop and the estimated walking time from that point. In addition, the app allows users to view the bus timetable, making it possible to check whether they can catch the last bus. Weather forecasts can also be accessed through the app. Furthermore, the app can be used to look up the names of mountains, flowers, and birds. For these functions, it is necessary for the beacon to be detected before the user reaches the point. In addition, some beacon installation points also serve as guidance at trail junctions, and if notifications are triggered only after passing trail junctions, there is a risk that users may become disoriented. Therefore, the target is for the beacon to be detected at least around a radius of 5 m, corresponding to 3.5 seconds in advance assuming a walking speed of 1.4 m/s. Additionally, measurements of GNSS positioning error taken in advance at each beacon installation point showed an average error of 5 m, which also serves as a basis for setting the detection radius. This condition is the same for both forested areas and open areas, and thus the detection radius is set to 5 m for both environments.

5 Experiments

To evaluate the proposed hybrid proximity detection method, we conducted experiments in two contrasting environments: the forested Senjogahara Nature Trail and a flat, open terrain. The Senjogahara trials assess real-world performance under forest canopy and variable GNSS conditions, while the flat-terrain trials establish performance bounds under ideal radio propagation.

5.1 Senjogahara Field Trials

Field experiments were carried out on November 12, 15, and 19 and on December 10, 2025. The numbers of participants were as follows: five on November 12 and 15 and four on November 19 and December 10. The participants were adult volunteers of both genders who agreed to participate in the study. Transportation to the study site was arranged by the research team; however, no financial compensation or other incentives were provided.

5.1.1 Experimental Setup

The evaluated methods were:

- BLE-only,
- GNSS-only,
- Proposed hybrid method triggered by two consecutive BLE receptions,
- Proposed hybrid method triggered by a single RSSI decrease.

A total of nine Android smartphones without cellular network contracts were used in the experiment. The smartphones used in the experiment are listed in Table 2. All devices ran the Android operating system and supported GPS, GLONASS, Galileo, QZSS, and BeiDou. None of the devices had an active mobile carrier subscription, and they were operated without internet connectivity, ensuring that no correction data or auxiliary positioning information was received.

Participants carried a smartphone running the *Oku-nikko Navi* application configured with one of the proximity-detection methods. On December 10, one participant carried two smartphones for comparison purposes. They walked along the Senjogahara hiking course beginning near Beacon No. 1, sequentially passing through beacons up to No. 21, and then returning to the vicinity of Beacon No. 1 as the endpoint. At each beacon, the participants either stopped walking when the proximity notification screen appeared or placed a marker on the ground to indicate that position. The straight-line distance between the beacon and the point where the notification appeared was

Table 2: List of smartphones used in the experiment

Model	OS Ver.	Nov. 12	Nov. 15	Nov. 19	Dec. 10
Google Pixel 6a (Charcoal)	16	—	GNSS	BLE	Hybrid (Rx×2)
Google Pixel 6a (Chalk)	16	BLE	—	GNSS	Hybrid (Rx×2)
Google Pixel 6a (Sage)	14	GNSS	BLE	—	Hybrid (decrease×1)
Google Pixel 7	15	BLE	GNSS	—	Hybrid (decrease×1)
Google Pixel 7a	16	GNSS	BLE	—	Hybrid (decrease×1)
Nothing CMF Phone 1	15	BLE	—	GNSS	Hybrid (Rx×2)
SONY Xperia 10 IV	14	—	GNSS	—	Hybrid (Rx×2)
Motorola moto g64y 5G	15	—	—	GNSS	—
Motorola motorola edge50s pro	15	—	—	—	Hybrid (decrease×1)

Note: "—" indicates that the device was not used on the corresponding date.

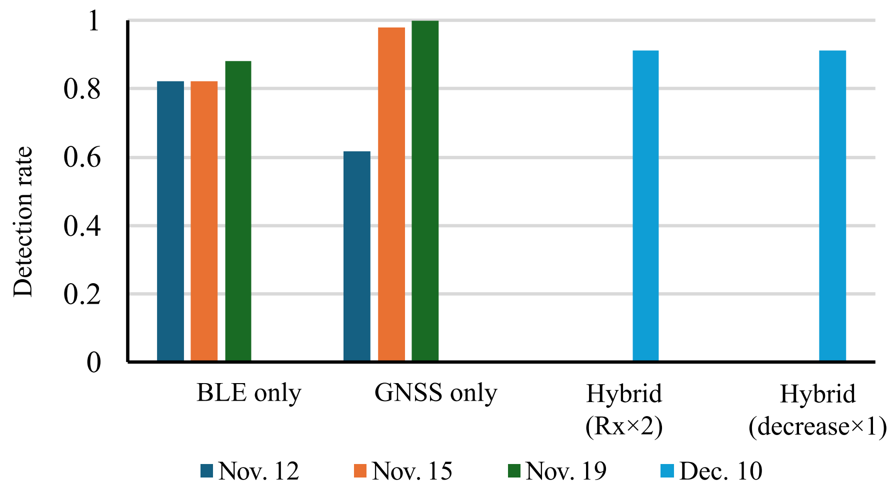

Figure 9: Signal detection rate in Senjogahara.

then measured with a tape measure and recorded as the positioning error d. The beacon detection rate R_{detect} for each method was defined as follows:

$$R_{\text{detect}} = \frac{N_{\text{detect}}}{N_{\text{total}}} \quad (3)$$

where, N_{detect} is the number of successful beacon detections and N_{total} is the total number of trials. At the end of each experiment, the battery consumption of the application on each device was recorded.

5.1.2 Results

Figure 9 presents the detection rate R_{detect} for each method across the four experimental days. The GNSS-based method achieved a detection rate of 0.62 on November 12, which is substantially lower than the rates observed on the other experimental days and those obtained by the alternative methods. These results suggest that some form of GNSS degradation occurred on that day. Therefore, in the following analysis, we report GNSS results both with and without the data from November 12.

Figure 10 summarizes the average distance errors. The error bars in the figure indicate the standard deviation. Table 3 reports the average errors and detection rates. The BLE-only method yielded an error of 58.33 m, whereas the GNSS-only method resulted in errors of 3.62 m (including

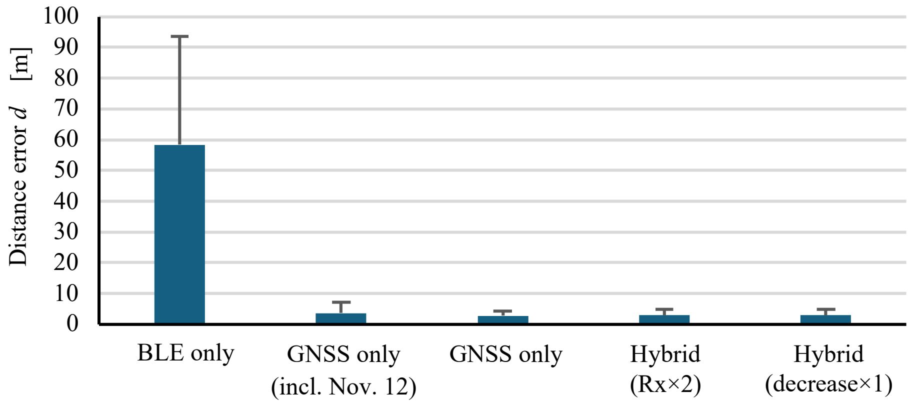

Figure 10: Average error by method in Senjogahara.

November 12) and 2.71 m (excluding November 12). The proposed hybrid methods yielded errors of 2.92 m and 2.95 m, respectively.

Table 3: Average positioning error, standard deviation, and detection rate in Senjogahara

Method	Positioning error (m) average	SD	R_{detect}
BLE-only	58.33	35.39	0.83
GNSS-only(incl. Nov. 12)	3.62	3.57	0.90
GNSS-only	2.71	1.65	0.99
Hybrid (received twice)	2.92	2.06	0.91
Hybrid (single decrease)	2.95	1.82	0.91

Figure 11 presents the proximity detection errors for each beacon point. The results of the BLE-only method are omitted because an examination of individual beacon locations revealed that the BLE-only method produced the largest errors at nearly all sites and exhibited error characteristics markedly different from those of the other methods. From Figure 11, it can be observed that the hybrid method yields smaller errors than the GNSS-only method at beacon No. 4, 7, 11, 15, 17, and 20. In particular, locations 11, 17, and 20 are areas with dense tree cover, and the hybrid method's superior performance in such environments is noteworthy.

For beacon point No. 5, the distance data for the Hybrid method are missing because no radio signals were transmitted from the beacon on the day of the experiment. Beacon No. 8 was malfunctioning on the day of the experiment and was not operational; therefore, no data were obtained for this beacon. For the open-area beacons (No. 4, 6, 7, and 9), GNSS-only and Hybrid show nearly the same level of error, except for No. 4, where there are a few trees nearby. For No. 4, the Hybrid method had a smaller error than GNSS. In forested areas, the locations where GNSS has smaller errors and the locations where Hybrid has smaller errors are evenly split. However, in locations with denser tree cover within the forested area — namely No. 11, 15, 17, 18, 19, 20, and 21 — one of the Hybrid methods yields the minimum error.

Figure 12 shows the average battery consumption per hour. The battery consumption ratios were comparable across all methods, with no substantial differences observed.

Figure 13 illustrates an example in which the proposed method failed to correctly identify the closest point due to large GNSS positioning errors. The red line indicates the hiking trail, while the blue pins represent the GNSS-estimated positions. In this example, the estimated positions deviate substantially from the actual trail both before and during the closest-point decision. Because the GNSS error was large, the estimated positions did not enter the 5 m threshold near the beacon,

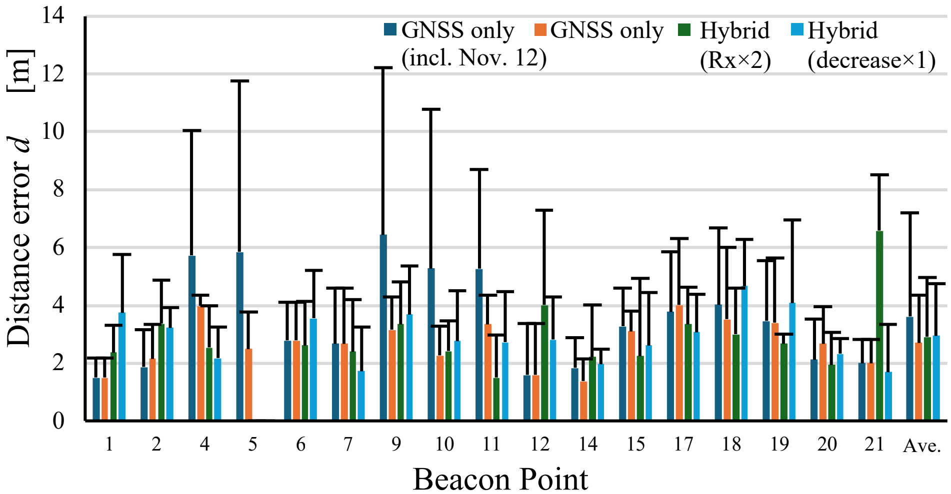

Figure 11: Average error by method in Senjogahara for each beacon.

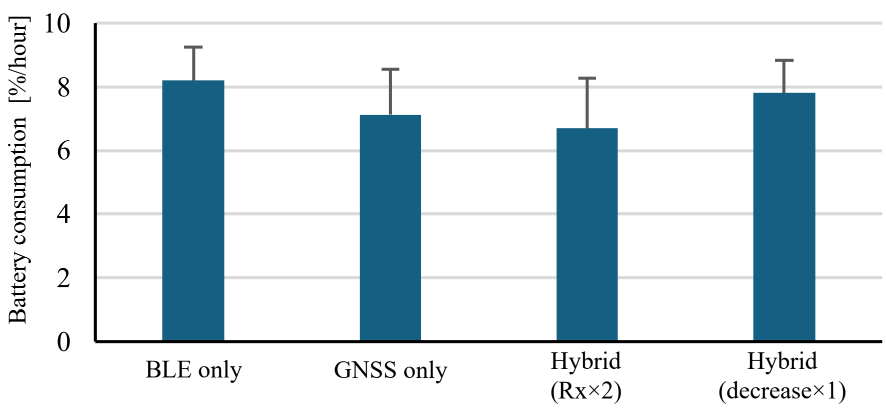

Figure 12: Battery consumption in Senjogahara.

resulting in a delayed closest-point declaration despite successfully receiving BLE signals.

Figure 14 shows the time-series GNSS distance to the beacon and the time-series BLE RSSI values around the proximity detection event. In this case, at around 12:50:55, when the GNSS distance reached 5 m and the gate-in event was triggered, the RSSI decreased immediately afterward, causing the closest-point decision to occur prematurely, before the user actually passed the beacon. Furthermore, even before this point, the RSSI repeatedly fluctuated between increases and decreases, indicating that the BLE signal was unstable.

5.1.3 Solar Flare Disturbance

In the GNSS-only method, the detection rate on November 12 dropped markedly to 0.62. This degradation is likely attributable to the X5.1-class solar flare that occurred on the same day. On November 12, large-scale geomagnetic disturbances and ionospheric storms caused by an X-class solar flare were reported by the National Institute of Information and Communications Technology (NICT) [17]. In addition, the Geospatial Information Authority of Japan (GSI) announced that general-purpose GNSS exhibited increased positioning errors on the same day [18]. Based on these observations, it is reasonable to infer that the solar flare was the primary cause of GNSS accuracy degradation in Senjogahara on that day.

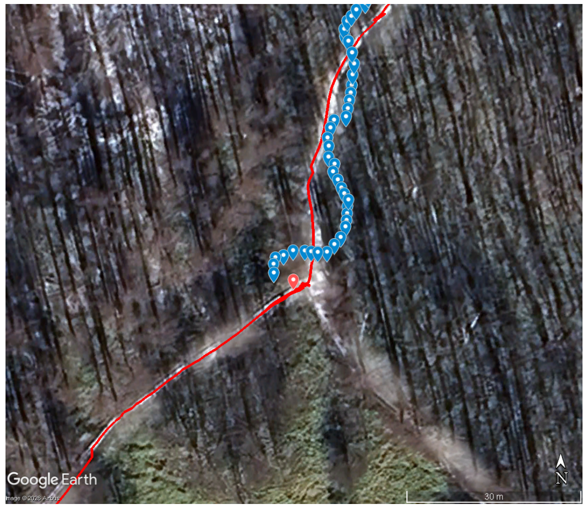

Figure 13: Example in which the proposed method failed to identify the closest point due to large GNSS positioning errors. The red line indicates the hiking trail, and the blue pins represent the GNSS-estimated positions (Beacon No. 12 on December 10).

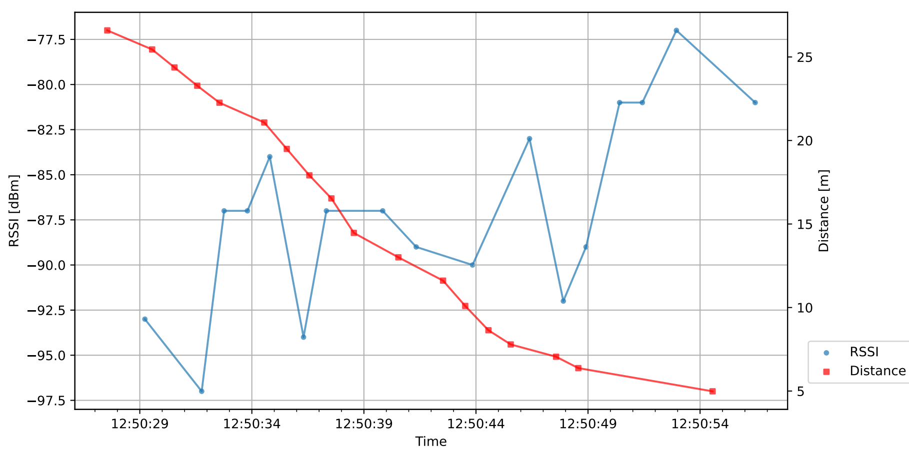

Figure 14: BLE RSSI changes and GNSS distance around the proximity detection event.

On November 12, the estimated positions drifted by an average of approximately 7 m off the trail, accompanied by a reduced GNSS fix success rate and substantially larger errors than on the other experimental days. Such behavior is consistent with prior reports indicating that ionospheric disturbances induced by X-class solar flares can significantly increase GNSS positioning errors [19].

Figure 15 shows the GNSS positioning errors observed at the nearby GEONET station “Kuriyama,” comparing a flare-free day (2025/09/09) with the day on which the X5.1-class solar flare occurred (2025/11/12). The results indicate that the errors on November 12 increased substantially, with north–south deviations exceeding 30 m. Moreover, the period during which large errors were recorded overlaps with the experimental observation window in this study, suggesting that the solar flare exerted a significant influence on GNSS performance on that day.

Figure 16 presents boxplots of the GNSS positioning errors obtained during walking with GNSS-enabled devices. The whiskers represent the minimum and maximum values, excluding outliers. The first four digits of each label denote the measurement date, and the subsequent characters indicate the device name. The two boxplots on the left for November 12 exhibit a substantially wider distribution than those for the other days, indicating markedly larger errors.

In fact, the mean errors were 2.00 m on November 19 and 2.96 m on December 10, whereas the

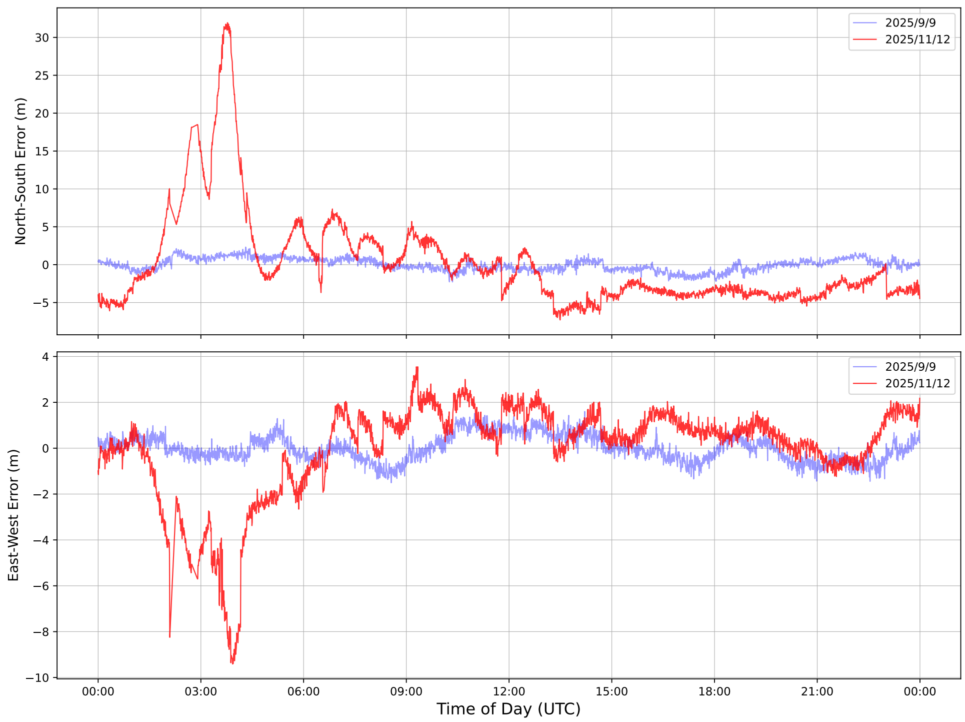

Figure 15: GNSS positioning errors at the Kuriyama GEONET station. Plotted using the data from Ref. [20].

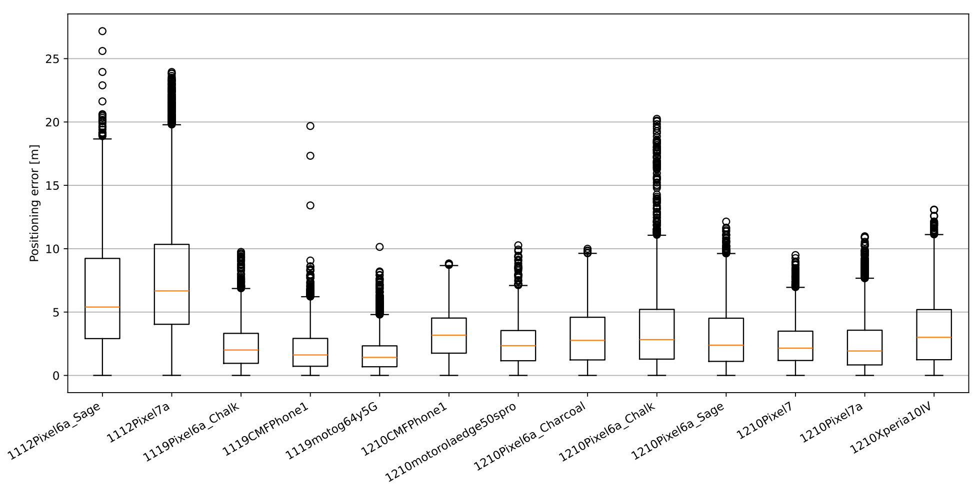

Figure 16: GNSS positioning errors during walking in the Senjogahara nature trail (the first four digits indicate the experiment date, and the subsequent letters represent the device name).

mean error on November 12 reached 7.01 m. In addition to the increased mean error, the error distribution on November 12 broadened significantly, further corroborating that GNSS exhibited anomalous behavior on that date.

5.1.4 Discussion

When the GNSS outage day (November 12) was excluded, the GNSS-only method achieved the lowest average error under normal conditions. Several factors may explain this behavior, including

GNSS positioning errors, deviations from the BLE signal reception patterns assumed by the proposed method, and cases in which certain smartphones failed to receive BLE signals that were successfully detected by other devices.

However, as shown in Figure 11, the hybrid method outperformed GNSS-only at several densely forested beacon locations (11, 15, 17, 18, 19, 20, and 21), demonstrating its robustness under canopy-induced GNSS degradation.

Figures 13 and 14 illustrate two failure modes. Figure 13 shows that large GNSS errors can prevent the system from entering the 5 m gating threshold, causing delayed detection. Figure 14 demonstrates that RSSI fluctuations can trigger premature activation. These results indicate that the fixed 5 m threshold may be suboptimal under severe GNSS degradation, and that BLE-based triggers are sensitive to signal instability in outdoor environments.

During the solar flare event on November 12, the GNSS-only detection rate dropped to 0.62, which was substantially lower than the detection rates of 0.91 achieved by the hybrid methods on the other experimental days. Overall, the Senjogahara trials indicate that while GNSS-only achieves the best accuracy under normal conditions, the hybrid approach offers superior robustness at densely forested locations. The drop in GNSS-only detection rate on the solar flare day further suggests that the hybrid approach may also be beneficial under geomagnetic disturbances, although a direct comparison under such conditions remains as future work.

5.2 Flat Terrain Trials

To complement the evaluations conducted in forest environments, an additional experiment was performed on flat terrain where GNSS signals are expected to be stable and unobstructed. The purpose of this experiment was to clarify the upper-bound performance and operational limitations of the proposed proximity detection method under ideal radio conditions, with minimal multipath effects and BLE signal attenuation.

5.2.1 Experimental Conditions

The experiment was conducted from February 2 to 6, 2026. It was conducted on an open university rugby field with no surrounding obstacles. Figure 17 shows the experimental setup. A BLE beacon was mounted on a tripod at a height of 1 m and configured with a transmission power of +4 dBm and an advertising interval of 1500 ms. Two Google Pixel 6a smartphones running Android 16 were used as receiver devices.

A single adult participant walked in a straight line from a starting point located 100 m away from the beacon toward its position. When the proximity notification screen appeared on the smartphone, the participant stopped walking. The straight-line distance between the stopping point and the actual beacon location was recorded as the positioning error. The GNSS proximity threshold for the gating mechanism was set to $r = 5$ m. The flat-terrain trial evaluated the same four proximity-detection methods as those used in the Senjogahara experiments. Each method was tested with 50 trials.

5.2.2 Results

Table 4 shows the experimental results. Because the BLE advertising interval was relatively long, the BLE-only method showed variability in the detection timing depending on the participant's walking speed. In contrast, the GNSS-only method demonstrated high detection stability due to the unobstructed sky view and favorable satellite geometry.

Among the proposed methods, Hybrid (received twice) exhibited substantially smaller errors than the BLE-only method and slightly smaller errors than the GNSS-only method. It also maintained a detection rate close to 1.

By contrast, Hybrid (single decrease) exhibited an error magnitude comparable to that of the GNSS-only method; however, its detection rate was lower. This was primarily because transient decreases in RSSI were observed even while the participant was approaching the beacon, causing the BLE trigger to activate at inappropriate locations. In addition, there were cases in which RSSI

(a) BLE beacon and stand

(b) Field setup

Figure 17: Experimental equipment and experiment field setup. (a) BLE beacon on tripod. (b) Test field with starting positions (blue) and beacon location (red).

Table 4: Average positioning error, standard deviation, and detection rate on flat terrain (50 trials per method)

	Positioning error (m)		
Method	average	SD	R_{detect}
BLE-only	31.24	15.03	1.00
GNSS-only	3.11	0.85	1.00
Hybrid (received twice)	1.90	1.18	0.98
Hybrid (single decrease)	3.11	1.40	0.82

did not decrease monotonically even when the participant was moving away from the beacon, as well as cases in which the beacon signal was not received at all. These factors also contributed to the reduced detection rate. These results indicate that the assumption of a monotonic decrease in RSSI after the closest point does not necessarily hold in real BLE environments. Since the advertising interval was set to 1500 ms—considerably longer than typical BLE configurations—the timing of BLE receptions became highly sparse, amplifying the instability of BLE-based triggers. This confirms that the assumptions of the analytical model in Section 4.2 do not hold in practice.

5.2.3 Discussion

The flat-terrain trial provides the following insights:

- In environments where GNSS operates stably, the GNSS-only method delivers high accuracy and a perfect detection rate.
- The BLE-only method is susceptible to walking-speed-dependent timing variations due to the long advertising interval.
- Hybrid (received twice) effectively suppresses BLE instability and provides stable short-range refinement, consistent with the results observed in forest environments.
- Hybrid (single decrease) is sensitive to non-monotonic RSSI behavior and long advertising intervals, making it less reliable for robust detection.

These findings confirm that even in ideal outdoor environments, when the advertising interval is long, RSSI-gradient-based triggers alone are not sufficiently reliable, and BLE-based refinement is most effective when combined with stable, reception-count-based triggering.

6 Discussion

6.1 When Fusion Helps Most

Hybrid methods are useful under forest canopy. In our experimental field, when the transmit interval was long (approximately 1500 ms), the reception-count trigger (received twice) exhibited slightly higher reliability than the RSSI-decrease trigger.

6.2 Failure Modes and Mitigations

This section summarizes the major failure modes that influence the performance of the proposed proximity detection and positioning method in real-world environments, as well as the corresponding mitigation strategies derived from our experiments and existing knowledge.

First, GNSS drift can occur when horizontal accuracy deteriorates due to environmental factors in forested or urban areas. In such cases, adaptively increasing the threshold r is effective in preventing missed detections. To improve continuity, integrating inertial sensors or pedestrian dead reckoning (PDR) is also beneficial, as GNSS alone may fail to provide stable estimates.

Second, BLE reception misses may arise due to long advertising intervals or signal obstruction. When no signal is received within a predefined time window, switching to the GNSS-based closest-point estimation through a timeout mechanism is an effective fallback. Additionally, when a user approaches a beacon, the smartphone can advertise to trigger a high-rate transmission mode on the beacon side, further mitigating the impact of reception misses. This concept is presented as a future design option and was not implemented in the current system.

Third, the inherent randomness of RSSI is a fundamental challenge for BLE-based ranging. In particular, when the advertising interval is long, only a small number of RSSI samples can be obtained and the sampling interval becomes large, causing RSSI trends to be strongly influenced by noise and therefore unstable. This issue can be mitigated by employing trigger strategies based on multiple events rather than relying on a single RSSI change.

Finally, energy constraints are an important consideration, particularly in outdoor deployments. Duty cycling can be used to conserve power, keeping the transmission rate low under normal conditions and increasing it only when a user approaches. When feasible, upgrading solar panels or battery capacity further enhances operational robustness.

In summary, although a BLE–GNSS hybrid system is subject to several potential failure modes, combining appropriate mitigation strategies enables robust operation in diverse real-world environments.

6.3 Design Implications for Tourism Apps in Forest Areas

In environments where power availability and maintenance access are constrained, combining BLE and GNSS offers a practical balance. Ensuring system robustness requires continuous online health checks, such as verifying beacon availability and GNSS accuracy, and fallback mechanisms that can maintain guidance even when one of the modalities becomes impaired.

6.4 Answer to the Research Questions

Based on the experimental results obtained in both the Senjogahara forest environment and the flat-terrain trials, the research questions presented in the Introduction can be answered as follows.

RQ: Can a hybrid proximity detection framework that integrates GNSS-based coarse gating with BLE-based short-range refinement achieve more reliable and accurate proximity detection than GNSS-only and BLE-only approaches in forested and mountainous outdoor environments?

- **Effectiveness of the hybrid method.** In the Senjogahara trials, the proposed hybrid methods achieved average positioning errors of 2.92–2.95 m, which were comparable to the GNSS-only method under normal conditions. At several densely forested locations (e.g., beacon points

11, 15, 17, 18, 19, 20, and 21), the hybrid method outperformed GNSS-only, demonstrating its robustness under canopy-induced GNSS degradation. On November 12, the detection rate of the GNSS-only method dropped to 0.62 due to an X5.1-class solar flare. The hybrid method, which also incorporates GNSS measurements, was evaluated under nominal GNSS conditions and achieved a detection rate of 0.91.Although the hybrid method relies partly on GNSS and its performance may degrade under severe GNSS disturbances, the results under nominal conditions suggest that integrating complementary information has the potential to mitigate performance degradation caused by GNSS unreliability.

- **Limitations of BLE-only detection.** The BLE-only method exhibited large errors (58.33 m on average) due to long advertising intervals and significant RSSI fluctuations, indicating that BLE alone is unsuitable for accurate proximity detection in outdoor environments.

- **Comparison between BLE trigger mechanisms.** Among the two BLE trigger mechanisms, the reception-count trigger ("received twice") consistently produced more stable results than the RSSI-decrease trigger. In both Senjogahara and flat-terrain trials, the RSSI-decrease trigger was sensitive to non-monotonic RSSI behavior and yielded lower detection rates, while the reception-count trigger maintained stable performance even under fluctuating RSSI conditions.

In summary, the hybrid GNSS–BLE approach effectively addresses the limitations of single-modality proximity detection and provides robust performance across diverse outdoor environments.

7 Conclusion

In this paper, we proposed a GNSS-BLE hybrid proximity detection method for outdoor tourism applications in mountainous and forested environments. The proposed method combines GNSS-based coarse detection with BLE-based refinement to improve proximity detection under challenging conditions. The proposed method achieved a mean positioning error of 2.92 m in Senjogahara, where open areas and forested zones coexist, and 1.90 m in flat urban environments.

Through field experiments conducted in both open areas and forest environments in Senjogahara, we evaluated the performance of the proposed approach and compared it with BLE-only and GNSS-only methods. The results indicate that the hybrid approach achieves stable performance across different environments and maintains robustness even under degraded GNSS conditions, while providing smaller errors than BLE-only approaches and comparable accuracy to GNSS under normal conditions.

In addition, we analyzed the behavior of two BLE trigger mechanisms and discussed their characteristics under practical deployment conditions. We also presented implementation considerations for real-world systems, including constraints related to beacon operation and environmental variability. These findings suggest that the proposed approach is a viable option for supporting reliable location-based services in outdoor tourism scenarios.

Future work includes enhancing the reliability of outdoor proximity detection through improvements to beacon hardware — such as higher-efficiency solar panels and larger batteries — and applying machine-learning-based RSSI denoising techniques. Furthermore, integrating complementary positioning modalities, including pedestrian dead reckoning (PDR), is expected to further improve accuracy under forest canopy.

Acknowledgments

This work builds on field deployments and studies conducted in Senjogahara. We thank the staff, students, and collaborators who assisted with experiments and app development. This research is supported by JSPS KAKENHI Grant Number JP23H03649.

References

[1] Heather Kennedy-Eden and Ulrike Gretzel. A taxonomy of mobile applications in tourism. *E-review of Tourism Research*, 10(2):47–50, 2012.

[2] Paolo Barsocchi, Michele Girolami, and Davide La Rosa. Detecting proximity with bluetooth low energy beacons for cultural heritage. *Sensors*, 21(21):7089, 2021.

[3] Vicente Cantón Paterna, Anna Calveras Augé, Josep Paradells Aspas, and María Alejandra Pérez Bullones. A bluetooth low energy indoor positioning system with channel diversity, weighted trilateration and kalman filtering. *Sensors*, 17(12):2927, 2017.

[4] Fredrik Holmqvist and Abdulnaser Abdulfattah. Bluetooth low energy (BLE) 5.1 angle of arrival (aoa) measurements at submeter level. Master's thesis, Jönköping University, School of Engineering, June 2024.

[5] Nuno F. Paulino, Luís M. Pessoa, André Branquinho, and Edgar S. Gonçalves. Design and experimental evaluation of a bluetooth 5.1 antenna array for angle-of-arrival estimation. In *2022 13th International Symposium on Communication Systems, Networks and Digital Signal Processing (CSNDSP)*, pages 625–630, 2022.

[6] Nuno F. Paulino and Luís M. Pessoa. Self-localization via circular bluetooth 5.1 antenna array receiver. *IEEE Access*, 11:365–395, 2023.

[7] Kun Xiao, Fuzhong Hao, Weijian Zhang, Nuannuan Li, and Yintao Wang. Research and implementation of indoor positioning algorithm based on bluetooth 5.1 aoa and aod. *Sensors*, 24(14):4579, 2024.

[8] Felix Långberg and Jonas Thurborg. Design of a size reduced antenna array for angle of arrival (aoa) estimation for BLE 5.1. Master's thesis, Lund University, 2020.

[9] Chunxiang Wu, Yapeng Wang, Wei Ke, and Xu Yang. A dual-branch convolutional neural network-based bluetooth low energy indoor positioning algorithm by fusing received signal strength with angle of arrival. *Mathematics*, 12(17), 2024.

[10] Yongjie Yang, Hao Yang, and Fandi Meng. A bluetooth indoor positioning system based on deep learning with rssi and aoa. *Sensors*, 25(9), 2025.

[11] Trong-Thanh Han, Phuc Nguyen Dinh, Toan Nguyen Duc, Vu Nguyen Long, and Hung Dinh Tan. An efficient method for BLE indoor localization using signal fingerprint. *EAI Endorsed Transactions on Industrial Networks and Intelligent Systems*, 12(1), 2024.

[12] Mingfeng Li, Lichen Zhao, Ding Tan, and Xiaozhe Tong. BLE fingerprint indoor localization algorithm based on eight-neighborhood template matching. *Sensors*, 19(22):4859, 2019.

[13] Jiefan Huang, Yingyu Guo, Xuan Li, Ning Zhang, Jiang Jiang, and Guangyu Wang. Evaluation of positioning accuracy of smartphones under different canopy openness. *Forests*, 13(10):1591, 2022.

[14] Julián Tomaštík, Juliána Chudá, Daniel Tunák, František Chudý, and Miroslav Kardoš. Advances in smartphone positioning in forests: dual-frequency receivers and raw gnss data. *Forestry*, 94(2):292–310, 2021.

[15] Ali Broumandan, Isabelle Tremblay, and Sandy Kennedy. Impact of solar cycle 25 on gnss measurements: Analysis of ionospheric scintillation and positioning challenges. *Engineering Proceedings*, 88(1):21, 2025.

[16] Huan Luo, Yaxin Li, Jingxian Wang, Duojie Weng, Junhua Ye, Li-Ta Hsu, and Wu Chen. Integration of gnss and BLE technology with inertial sensors for real-time positioning in urban environments. *IEEE Access*, 9:11384–11396, 2021.

[17] Space Environment Laboratory, Electromagnetic Wave Propagation Research Center, Electromagnetic Research Institute. Multiple large solar eruptions occurred on the solar surface from november 9 to 14, 2025, and high-speed coronal gas ejection toward earth was confirmed. https://swc.nict.go.jp/report/topics/202511121600.html. Accessed Jan. 6, 2026 (in Japanese).

[18] Geospatial Information Authority of Japan (GSI). Impact of the november 12 solar flare on gnss positioning. https://www.gsi.go.jp/denshi/denshi65019.html. Accessed Jan. 6, 2026 (in Japanese).

[19] Yury Yasyukevich, Elvira Astafyeva, Artem Padokhin, Vera Ivanova, Semen Syrovatskii, and A. Podlesnyi. The 6 september 2017 x-class solar flares and their impacts on the ionosphere, gnss, and hf radio wave propagation. *Space Weather*, 16(8):1013–1027, 2018.

[20] Geospatial Information Authority of Japan (GSI). Electronic control point data provision service. https://terras.gsi.go.jp/. Accessed Jan. 6, 2026 (in Japanese).